



UNITED STATES  
NUCLEAR REGULATORY COMMISSION  
WASHINGTON, D.C. 20555-0001

July 3, 2001

MEMORANDUM TO: M. Wayne Hodges, Deputy Director  
Technical Review Directorate, SFPO

THROUGH: Earl P. Easton, Chief */RA/*  
Technical Review Section A, SFPO

FROM: Kimberly A. Gruss, Materials Engineer */RA/*  
Technical Review Section A, SFPO

SUBJECT: SUPPLEMENTARY INFORMATION SUPPORTING THE U.S.  
NUCLEAR REGULATORY COMMISSION'S REQUEST FOR  
ADDITIONAL INFORMATION TO THE NUCLEAR ENERGY  
INSTITUTE ON HIGH BURNUP FUEL CHARACTERISTICS

On May 18, 2001, a request for additional information (RAI) on the characteristics of high burnup fuel was transmitted to Lynette Hendricks of the Nuclear Energy Institute. The RAI followed the staff's, and Pacific Northwest National Laboratory's (PNNL), reviews of two Electrical Power Research Institute (EPRI) reports on high burnup fuel. These reports were TR-1001207 entitled "Creep as the Limiting Mechanism for Spent Fuel Dry Storage" and TR-1001281 entitled, "Fracture Toughness Data for Zirconium Alloys – Application to Spent Fuel Cladding in Dry Storage."

Attached for your consideration is supplementary information from (PNNL) related to the RAI questions. Attachment No. 1 is a list of references that contains creep rupture data that is being used to support the development of the NUREG/CR on cladding temperature limits. Attachment No. 2 is a summary of PNNL's review of EPRI's fracture toughness report (i.e., TR-1001281).

Attachments: 1. References Containing Creep to  
Rupture Data  
2. PNNL Review of EPRI TR-1001281

July 3, 2001

MEMORANDUM TO: M. Wayne Hodges, Deputy Director  
Technical Review Directorate, SFPO

THROUGH: Earl P. Easton, Chief (Original Signed by:)  
Technical Review Section A, SFPO

FROM: Kimberly A. Gruss, Materials Engineer (Original Signed by:)  
Technical Review Section A, SFPO

SUBJECT: SUPPLEMENTARY INFORMATION SUPPORTING THE U.S.  
NUCLEAR REGULATORY COMMISSION'S REQUEST FOR  
ADDITIONAL INFORMATION TO THE NUCLEAR ENERGY  
INSTITUTE ON HIGH BURNUP FUEL CHARACTERISTICS

On May 18, 2001, a request for additional information (RAI) on the characteristics of high burnup fuel was transmitted to Lynette Hendricks of the Nuclear Energy Institute. The RAI followed the staff's, and Pacific Northwest National Laboratory's (PNNL), reviews of two Electrical Power Research Institute (EPRI) reports on high burnup fuel. These reports were TR-1001207 entitled "Creep as the Limiting Mechanism for Spent Fuel Dry Storage" and TR-1001281 entitled, "Fracture Toughness Data for Zirconium Alloys – Application to Spent Fuel Cladding in Dry Storage."

Attached for your consideration is supplementary information from (PNNL) related to the RAI questions. Attachment No. 1 is a list of references that contains creep rupture data that is being used to support the development of the NUREG/CR on cladding temperature limits. Attachment No. 2 is a summary of PNNL's review of EPRI's fracture toughness report (i.e., TR-1001281).

- Attachments: 1. References Containing Creep to Rupture Data  
2. PNNL Review of EPRI TR-1001281

DISTRIBUTION:

NRC File Center NMSS r/f SFPO r/f PUBLIC

ADAMS: ML011840263

C:\KIMGRUSS\SFPO\HI BU FUELS\NEI MEETINGS\LTR-SUPPLM INFO.DOC

<b>OFC:</b>	SFPO	E	SFPO		SFPO						
<b>NAME:</b>	KGruss		EEaston		WHodges						
<b>DATE:</b>	7/3/01		7/3/01		7/ /01		/ /01		/ /01		

**C = COVER E = COVER & ENCLOSURE N = NO COPY OFFICIAL RECORD COPY**

## Attachment 1

### References Containing Creep to Rupture Data

1. Bouffieux, P. and N. Rupa. 2000. "Impact of Hydrogen Pick up on Plasticity and Creep of Unirradiated Zircaloy-4 Cladding Tubes," ASTM STP 1354, pp. 399-422, Twelfth International Symposium on Zirconium in the Nuclear Industry, American Society for Testing and Materials, West Conshohocken, Pennsylvania.
2. Chung, HM, FL Yaggee, and TF Kassner. 1987. "Fracture Behavior and Microstructural Characteristics of Irradiated Zircaloy Cladding," ASTM STP 939, 775-801, Zirconium in the Nuclear Industry: Seventh International Symposium, American Society for Testing and Materials, Philadelphia, Pennsylvania.
3. Goll, W, H Spilker, and EH Toscano. 2001. "Short-Time Creep and Rupture Tests on High Burnup Fuel Rod Cladding," J. Nucl. Mater., 289:3:247-253, Elsevier Science, Amsterdam, The Netherlands.
4. Limon, R, C Cappelaere, T Bredel, and P Bouffieux. 2000. "A Formulation of the Spent Fuel Cladding Creep Behaviour for Long Term Storage," Proceedings of the 2000 International Topical Meeting on LWR Fuel Performance, Vol. 2, 959-969, American Nuclear Society, La Grange Park, Illinois.
5. Mayuzimi, M and K Murai. 1993. "Post Irradiation Creep and Rupture of Irradiated PWR Fuel Cladding," Proceedings of Nuclear Waste Management and Environmental Remediation, 607-612, Prague Czech Republic.
6. Pankaskie, PJ. 1962. Creep Properties of Zircaloy-2 for Design Application, HW-75267, General Electric Company, Richland, Washington.

## Attachment 2

### PNNL Review of TR-1001281

#### 1.0 Fracture Toughness Correlation

The report describes a critical strain energy density (CSED) approach for estimating the fracture toughness of a material on the basis of uniaxial stress strain curves. PNNL has reviewed the approach and has applied the method on a trial basis to test how successfully it can be applied to both irradiated fuel clad and materials for which there is a good data base for tensile and fracture toughness properties.

#### 1.1 Background on SED Approach

The work of Professor George Sih at Leigh University is cited as the source of the CSED approach. Sih has long been a proponent of strain energy density as a useful parameter for various applications in the fracture mechanics field. Applications include criteria for establishing the preferred direction of crack growth in anisotropic materials and for structures with complex states of crack orientation and stress states. Applications to fiber reinforced composite materials have become relatively common. Applications (as described in the report) to elastic-plastic materials for predicting fracture toughness have been the topic of several publications, but have not seen much acceptance in the field of materials toughness testing.

The calculation of values for CSED is relatively simple, because it is just the integrated area under a stress-strain curve. Equations in the report describe a "first principals" approach that relates a CSED value for any material to the corresponding fracture toughness for the material. The CSED values and associated estimated fracture toughness are then compared with fracture/rupture data. This is where the approach becomes more complex because the CSED is most likely different for the different loading (stress) conditions. For example, creep versus tensile versus impact loads (fracture toughness) will have different stress and temperature states and different fracture mechanisms. Consequently, the approach requires a set of CSED data for a range of stress and temperatures that cover each of the applications that are to be addressed with the simple model. Dr. Rashid who proposes the used of CSED for nuclear fuel applications would say that CSED could apply to all of the above. That is, only uniaxial tensile data are needed to predict CSED for fracture toughness. If material behavior were this simple there would be no need for the field of fracture mechanics. In this regard, Dr. Rashid does acknowledge potential complications in a paragraph of the report.

Historically the field of fracture mechanics originated from the work during the 1940s and 50s by Dr. George Irwin at the Navel Research Laboratory because of unexpected structural failures for materials that should have exhibited ductile fracture behavior on the basis of their mechanical properties as measured by conventional tensile tests. It was however concluded that tensile properties were inadequate to characterize the susceptibility of materials to brittle fracture when cracks are present. In the case of ferritic steels it became clear that the state of stress near the crack tip was quite different than the stress state in a simple tensile test. The high degree of constraint to the yielding and relief of tensile stresses for the triaxial stress state near the crack tip was found to cause the initiation of brittle cleavage fractures at unexpectedly high temperatures. Having recognized the limitations of tensile tests, there was a rapid development of the field of fracture mechanics. The standardized tests for fracture toughness proved to be much more complex and costly than the standard tensile stress. Hence, much effort has gone

into the development of simple and economical tests and also to the formulation of theoretical models that can predict fracture toughness based on simple tensile tests.

The Charpy V-Notch (CVN) test has been widely used to characterize the toughness characteristics of engineering materials. It involves a small specimen size and a relatively simple testing procedure. The specimen of the CVN test has a notch geometry, and this produces some characteristics of the stress field of crack-like flaws. The test has been useful as a quality control test to ensure that specific lots of materials have adequate resistance to the propagation of brittle fractures. Comparisons of CVN data with data from fracture toughness tests have resulted a number of useful correlations that can estimate fracture toughnesses on the basis of measured CVN impact energies. No such correlations have been accepted to estimate fracture toughness on the basis of measure uniaxial tensile properties, although it is generally acknowledged that materials with high tensile ductilities will tend to have higher fracture toughness levels than materials with lower levels of tensile ductilities. The failure mechanisms for fracture are too numerous and complex to trust the accuracy of empirical correlations, other than over narrow ranges of materials and test conditions. In the case of ferritic steels the existence of a transition temperature for ductile versus brittle fracture has complicated the efforts to develop correlations. In the case of zirconium alloys, the effects of temperature are further complicated by the effects of hydrides on fracture toughness.

## 1.2 Application to Toughness Data for Ferritic Steels

The report presents an example application of the CSED criteria to aluminum alloys as shown by Figure 1-1 (Figure 5-2 of the report). The data on this plot show very good agreement between measured and predicted values for  $K_{IC}$ .

As part of PNNL's review, the CSED criterion was applied to a set of data for tensile and fracture properties of ferritic steels that was taken from Table 6.1 the Rolfe and Barsom book. Table 1-1 presents this data set along with predicted values of  $K_{IC}$  that were predicted using the equations of the report. Results of this exercise are shown by Figure 1-2. The agreement between predicted and measured values of fracture toughness is not nearly as good as for aluminum alloys. The report was not clear as to what measure of failure strain (reduction in area or tensile elongation) should be used. Calculations were therefore performed by three alternative methods: 1) strain based on elongation in a 1-inch gage length, 2) strain based on the reduction in area, and 3) the average strain of the first two methods. The best correlation was achieved by using an average of the two strain measures. The most conservative estimates came from using a strain based on the elongation in the 1-inch gage length.

Predicted and measured toughness values for the ferritic steels can differ by a factor of two rather than by ten percent or less as was the case for aluminum alloys. Given the assumptions made in developing the CSED equations, the observed scatter in predicted values is not surprising. The almost total lack of scatter for the aluminum alloy is perhaps more surprising. The apparently good agreement for aluminum could be the result of fine-tuning of the inputs to the model (use of reductions in area versus elongations) or assumptions such as the assigned value for the critical plastic zone size.

Figure 1-3 is reproduced from page 3-11 of EPRI Report 1001207, and shows CSED values measured from a number of tests of irradiated and hydrided fuel cladding. The extent of the exposure is expressed in terms of the thickness of the oxide layer on the external surface of the clad. The data show a wide scatter in the measured CSED, but with a clear trend of reduced energy levels as the clad experiences high levels of corrosion. PNNL used the CSED data of

Figure 1-3 and the predictive equations in the EPRI report to predict fracture toughness values. These values are shown by Figure 1-4 along with recommended estimates from the report for fracture toughness as by fracture toughness tests. In order to produce this plot it was necessary to relate hydrogen levels (PPM) to oxide thickness. The solid data points with the indicated hydrogen levels give the assumed correlation. The correlation is subject to large uncertainties and should be updated as better estimates become available. Figure 1-4 does however provide some useful insights. In general, the estimates of fracture toughness from the CSED approach are more conservative than the estimates based on data from fracture mechanics tests, although in a few cases the CSED approach gives higher fracture toughness levels than the conservative curve from the toughness data. This would be expected because the CSED curves are based on tensile and burst tests of high burnup cladding, i.e., with non-uniform hydrides, while the fracture toughness data are from clad with uniformly distributed hydrides (artificially induced). In general, the data show that high burnup cladding with non-uniform hydrides seems to have lower ductility than cladding with uniform hydrides, and materials with lower ductility generally have lower fracture toughness than those with higher ductility. Note that the scatter in CSED estimates is large and similar to the scatter noted in the data from fracture toughness tests. The figure appears to demonstrate that spalled cladding has much lower fracture toughness than non-spalled cladding at equivalent oxidation and hydrogen pickup.

The present review indicates that the correlation to be expected for clad materials would likely be more similar to that shown in Figure 1-2 for ferritic steels rather than the remarkably good correlation seen for aluminum alloys. The CSED method could nevertheless be useful if it is properly calibrated using fracture toughness data for clad materials. The uncalibrated predictions for the toughnesses of ferritic steels and fuel clad are accurate within about factor of two, which shows the merits of the CSED approach. Applications of the CSED approach could be analogous to the common use of Charpy impact energies (CVN) to estimate fracture toughness values. The CSED method could allow a relatively simple test to estimate the toughness for specific heats of materials or in the case of cladding to evaluate materials exposed to various levels of irradiation and or hydrogen concentrations.

### 1.3 Summary and Conclusions

The CSED approach, as has been acknowledged in the EPRI report, does not provide a replacement for tests to measure fracture toughness. More work is needed to calibrate the CSED approach to provide adequate estimates of fracture toughness levels. Nevertheless, with adequate calibration and validation the CSED method could be a useful supplement to fracture toughness testing. For example, correlations of CSED with fracture toughness could permit structural integrity evaluations of irradiated and hydrided fuels to be performed in situations where only limited data on tensile properties are available. The CSED approach could also be used to identify materials and conditions for which additional fracture toughness tests are needed. Based on the lack of applicable high burnup fracture mechanics data, i.e., with non-uniform hydrides, it is difficult to assess the level of conservatism that should be used to calculate the fracture toughness with the current CSED approach.

MATERIAL	YIELD KSI	YIELD Mpa	TENSILE KSI	TENSILE Mpa	ELONGATION % IN 1-INCH	REDUCTION IN AREA %	ROLFE BARSOM KIC KSI -ROOT INCH	STRAIN BASE ON RED AREA DELTA-L/Lo	STRAIN BASE ON ELONGATION DELTA-L/Lo	TOUGHNESS BASED ON REDUCTION AREA KIC KSI-SQRT(INCH)	TOUGHNESS BASE ON ELONGATION KIC KSI-SQRT(INCH)	BASED ON AVERAGE OF REDUCTION AREA AND ELONGATION KIC KSI-SQRT(INCH)
A517-F, AM	110	759	121	834	20.0	66.0	170	1.94	0.20	215	69	160
4147, AM	137	945	154	1062	15.0	49.0	109	0.96	0.15	169	66	128
HY-130, AM	149	1028	159	1097	20.0	68.4	246	2.16	0.20	264	80	195
4130, AM	158	1090	167	1152	14.0	49.2	100	0.97	0.14	182	69	137
12NI-SCR-3MO, AM	175	1207	181	1248	14.0	62.2	130	1.65	0.14	250	72	184
12NI-SCR-3MO, VIM	183	1262	191	1317	15.0	61.2	220	1.58	0.15	250	76	185
12NI-SCR-3MO, VIM	186	1283	192	1324	17.0	67.1	226	2.04	0.17	286	82	211
18NI-8CO-3MO 200 GR	193	1331	200	1379	12.5	48.4	105	0.94	0.13	198	71	149
18NI-8CO-3MO 200 GR	190	1310	196	1352	12.0	53.7	112	1.16	0.12	218	69	162
18NI-8CO-3MO 190 GR	187	1290	195	1345	15.0	65.7	160	1.92	0.15	278	77	204
18NI-8CO-3MO 250 GR	246	1697	257	1772	11.5	53.9	87	1.17	0.12	249	77	184

**Table 1-1 Trial Application of Critical Strain Energy Density to Data for Ferritic Steels**

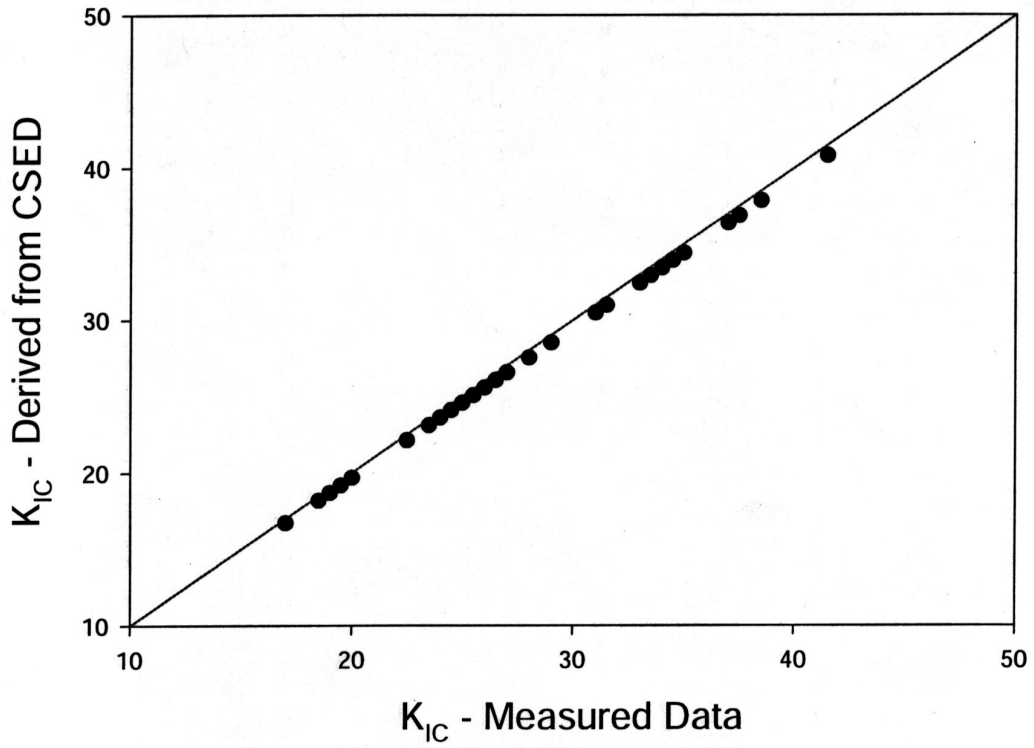
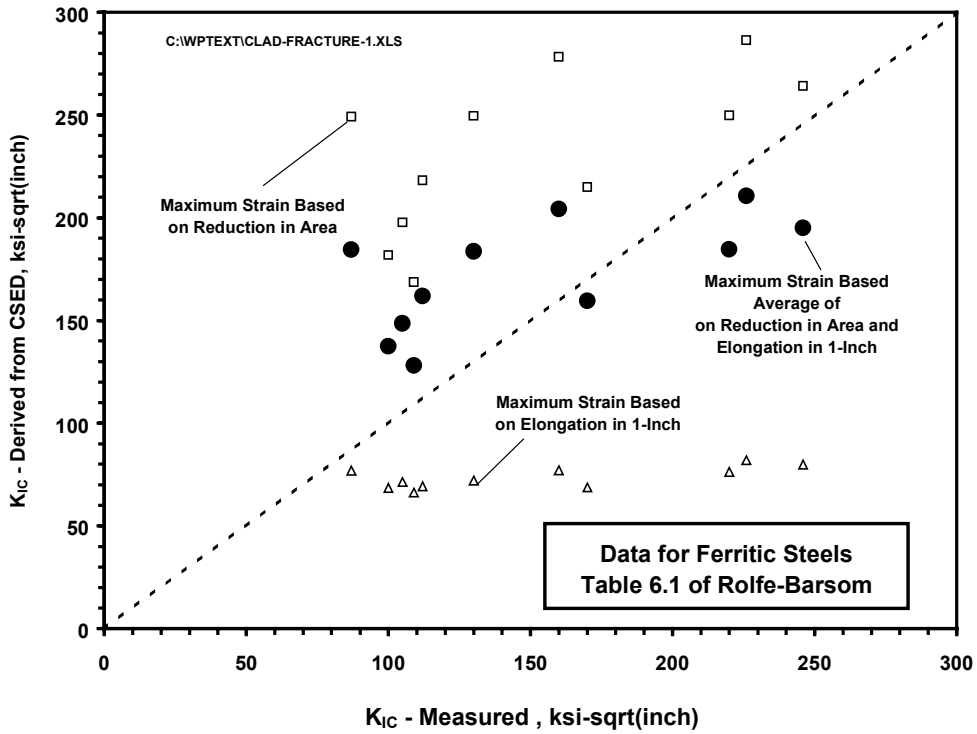
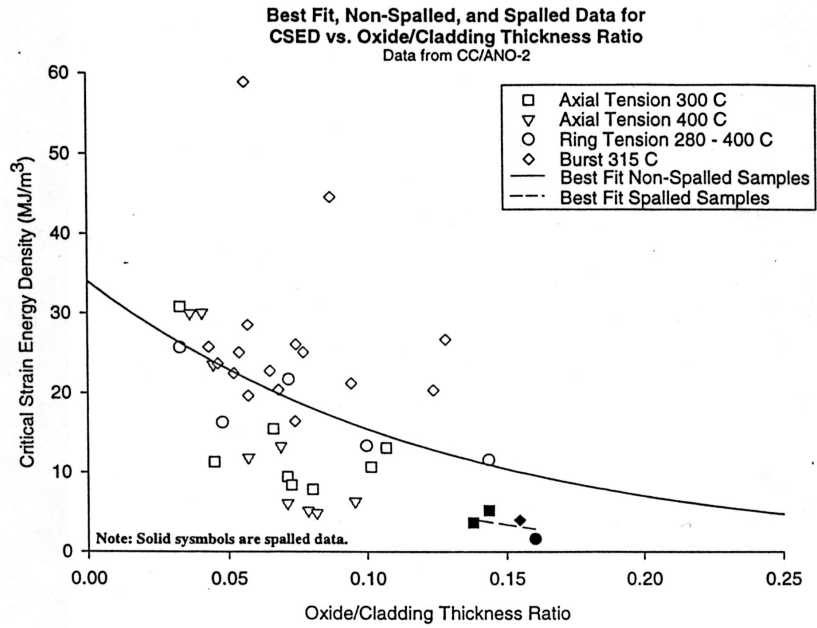


Figure 1-1 Application of CSED Approach to Aluminum Alloys (Figure 5-2 of Report)



**Figure 1-2 Trial Application of Critical Strain Energy Density Methodology to Data for Ferritic Steels**



**Figure 1-3 Values of CSED from EPRI Report 1001207)**

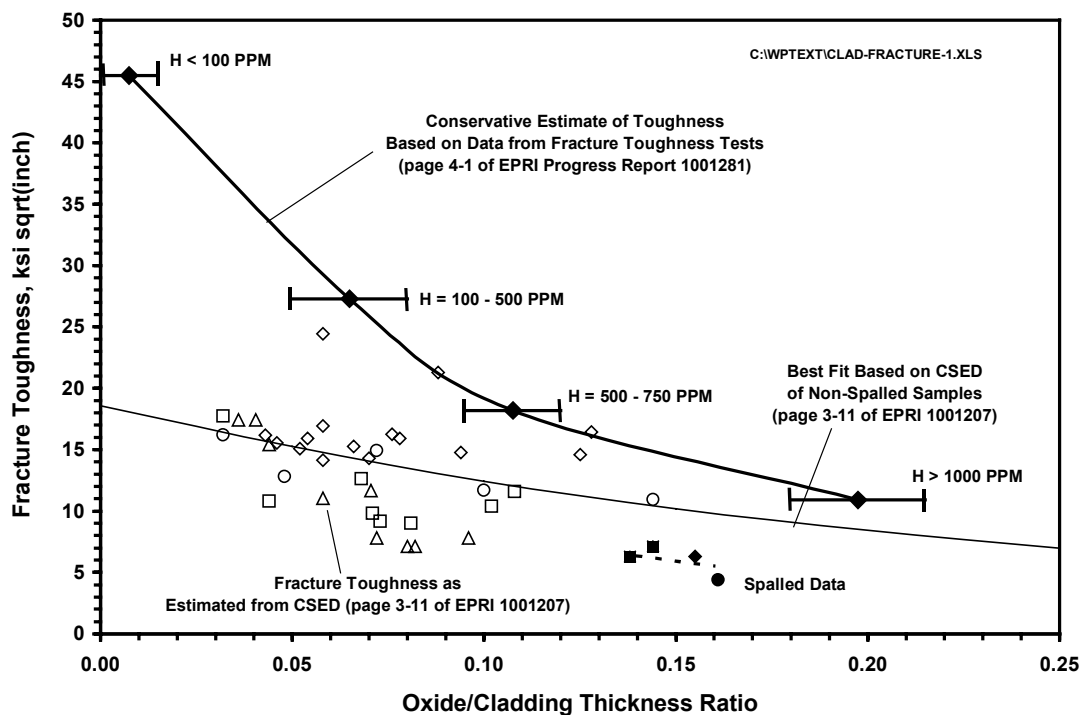


**Figure 1-4 Comparison of Fracture Toughness of Clad as Predicted by CSED Approach with Clad Toughness Measured by Fracture Toughness Tests**

## 2.0 Dynamic Propagation of Axial Cracks

Failures of fuel clad have occurred during reactor operation resulting in long axial cracks that have essentially extended the full lengths of fuel rods. These fractures have been driven by pellet-clad interactions, which operate over the full length of the fuel rod, such that an initially local rupture can propagate down the full length of a tube. Therefore, concerns have been expressed whether a similar mode of failure could produce such fractures during the storage of spent fuel, particularly for high burnup fuel with highly embrittled and hydrided clad materials. While mechanism of pellet-clad interaction is not relevant for the storage phase of spent fuel, high hoop stresses from internal pressures from fission gases offers an alternative driving mechanism that could cause long axial fractures in cladding. The discussion below describes an evaluation by PNNL that addresses the potential for such fuel failures during dry storage. The evaluation applies data and equations available from the literature for the propagation and arrest of axial cracks in gas transmission pipelines.

Figure 2-1 shows the tube geometry and pressure loading of concern to clad integrity. This figure was taken from a discussion of crack propagation in gas transmission pipelines (Kanninen and Popelar 1985; McGuiarre et al 1980). In the case of steel pipelines, there have been accidents that resulted in axial fractures that have run in an uncontrolled fashion for several miles. The question is whether a similar mode of fracture could occur in zirconium fuel rods. In the case of pipelines, the fractures first start in a short length of the pipeline that has been degraded by corrosion, cracking, and/or from some unusual load (impact by earth moving equipment). Local ruptures in pipelines have then extended beyond the locally degraded length and continued to grow under the action of the internal pressure at speeds of 100s of feet per second. In other cases the axial cracks have arrested with the rupture limited to only a short length of the pipeline. The gas pipeline industry has performed many full-scale tests and has developed fracture mechanics models to identify the factors that contribute to the arrest of running axial cracks. The basic assumption is that some local condition first causes an axial crack to grow rapidly. The following factors have been identified as important to the potential for crack arrest:

1. cracks will arrest if the velocity of the depressurization wave down the length of the pipe is greater than the velocity of axial crack propagation,
2. depressurization waves travel at the speed of sound in the contained gas,
3. the velocity of crack propagation can be very high for low toughness materials, but is still limited to some predictable fraction of the speed of sound in the pipe material,
4. the velocity of crack propagation is significantly reduced for materials with higher levels of fracture toughness,
5. the rate of crack propagation is a function of pipe dimensions; the velocity becomes slower as the ratio of the wall thickness to the diameter becomes smaller.

The following analysis will use data and models developed for gas pipelines to predict whether it is theoretically impossible for an axial split to extend more than a few tube diameters before the internal pressure is relieved to the extent that the needed driving force for crack propagation is lost. This analysis will take into account the sonic velocity of the confined fission product gases, fracture properties of uniformly hydrided clad, and the clad dimensions (diameter and thickness).

The following differences between gas transmission pipelines and fuel clad can be identified :

1. the diameters of the pipeline and clad differ by a factor of about 80, and this difference will make it more likely for cracks to arrest in the fuel clad,
2. the diameter to thickness ratio is about 20 for the clad versus a ratio of about 90 for the pipeline, and this difference will make it less likely for cracks to arrest in the fuel clad,
3. the pipeline is pressurized with natural gas (methane) versus a mixture of helium, xenon and krypton for the clad; the differences in sonic velocities for the two gas compositions are addressed below,
4. the fuel rod is filled with fuel pellets leaving only a thin outer annulus and a smaller plenum without pellets for the gas volume versus a pipe that is entirely filled with gas; although the very small gas volume of the fuel rod is expected to contribute to the arrest of cracks in the clad, a quantification of the effect was beyond the scope of the preliminary assessment that is described below,
5. the fracture toughness of the fuel clad materials can be less than the toughnesses of the materials used to fabricate gas pipelines, and this difference will make it less likely for running cracks to arrest in the clad compared to cracks in the pipeline situation.

The following evaluations quantify some of the trends listed above.

Kanninen and Popelar (1985) give the following equation for the limiting velocity for the propagation of an axial crack in a pipe

$$V_{\lambda} = 0.75 C_o (h/R)^{1/2}$$

where

h = wall thickness (0.41 inch for pipeline and 0.024 inch for clad)  
R = radius (17.6 inch for pipeline and 0.21 inch for clad)  
 $C_o = \text{longitudinal wave speed} = (E/\rho)^{1/2}$   
E = elastic modulus ( $30 \times 10^6$  psi for steel and  $13.9 \times 10^6$  psi for clad)  
 $\rho = \text{density}$  (0.283 lb/in<sup>3</sup> for steel and 0.23 lb/in<sup>3</sup> for clad)

Figure 2-2 from Kanninen and Popelar (1985) compares velocities for the gas pipeline situation.

The speed of sound in steel and zirconium alloys are calculated as

Steel:  $C_o = 16,400$  ft/sec,

Zirconium:  $C_o = 12,700$  ft/sec,

and the limiting speed of crack propagation in the steel pipeline versus the fuel clad is

Steel:  $V_{\lambda} = 1,877$  ft/sec,

Zirconium:  $V_{\lambda} = 3,200 \text{ ft/sec}$  .

The speed of sound in methane gas has a handbook value is 1,410 ft/sec, which indicates that for pipelines the speed of the depressurization wave is only slightly less than the limiting crack velocity. Therefore the evaluation shows a potential for the unarrested growth of long cracks for the pipeline conditions. The condition for crack arrest is not met for a very brittle steel, although the slower crack velocities for higher toughness steels can result in crack arrest.

The speed of sound for the gas mixture of the spent fuel can be calculated using the estimated density of the gas mixture and the temperature of the fuel during storage. The assumed molecular composition of the gas mixture was taken to be 37 percent helium, 53 percent xenon and 10 percent krypton, with the corresponding molecular weights being 2, 54 and 36. Based on a weighted average of the of these molecular weights the calculation gives a value of 32.96 compared to a molecular weight of 16 for methane. A calculation has also accounted for the effect of a temperature of 280 °C for the spent fuel compared to room temperature for the gas pipeline, by relating the speed of sound to the square root of the absolute temperature. This gave a following estimates of sonic velocities

Methane at RT:  $V_s = 1,410 \text{ ft/sec}$

Spent Fuel at 280 °C:  $V_s = 1,350 \text{ ft/sec}$

The ratio of the depressurization velocity to the limiting crack velocity is then

Pipeline at RT:  $V_s / V_{\lambda} = 1,410 / 1,877 = 0.75$

Spent Fuel at 280 °C:  $V_s / V_{\lambda} = 1,350 / 3200 = 0.42$  .

Based on simple considerations of sonic velocities, it is concluded that cracks are less likely to arrest in the fuel clad than in the pipeline. However, this conclusion does not account for potentially mitigating effects of fracture toughness, diameter of the clad versus pipeline, and potentially significant effect of very small confined gas volume because the fuel pellets occupy most of the volume inside the fuel rod.

The effect of fracture toughness is predicted by the following equation developed from correlations of data from full-scale tests on gas pipelines (McGuire 1980)

$$(CVN)_{\min} = 500 p_L^{4/3} Y^{2/3} R^{19/12} h^{-1/4} / E$$

where

CVN = minimum value of Charpy impact toughness for crack arrest (ft-lb)

$p_L$  = Internal Pressure, ksi

$Y$  = Yield Strength, ksi

$R$  = Radius, inch

$h$  = Wall Thickness, inch

$E$  = Elastic Modulus, ksi.

This equation was applied to address the issues of material toughness and diameter (size effect) as they influence the potential for crack arrest. Calculations were performed for the radius to thickness ratio of fuel clad ( $R/t = 0.21/0.024 = 8.75$ ) and for the material properties of gas pipelines (steel with  $Y$  and  $E$  equal to 70 ksi and 30,000 ksi). The gas pressure was assumed to be 1.4 ksi. The objective was to make an order of magnitude estimate of the fracture toughness levels needed to arrest a crack if the pipe diameter were reduced to dimensions characteristic of a fuel rod. It was recognized that this approach required a large extrapolation of the above empirical equation away from the test conditions for which the equation was developed. The results should therefore be used only in a qualitative manner.

Figure 2-3 shows the result of the calculations in terms of both CVN impact energies and the corresponding values of fracture toughness  $K_{IC}$ . The fracture toughness was correlated to the CVN values by an equation given in Rolfe and Barsom for the temperature transition region ( $K_{IC}^2/E = 5 \text{ CVN}$ ). A very significant size effect is shown by Figure 2-2. Whereas a pipeline with a radius of 17 inch would require a minimum toughness of about 80 ksi√inch to ensure crack arrest, the required toughness is reduced to about only 3 ksi√inch if the pipe size is reduced to the dimensions of a fuel rod. This minimum toughness for crack arrest is less than the minimum toughness of 5 to 10 ksi√inch estimated in the NEI report for irradiated and uniformly hydrided Zircaloy clad. The issue here is that uniformly hydrided Zircaloy (used to establish the minimum fracture toughness) appears to have higher ductility than observed in high burnup cladding that is non-uniformly hydrided (based on tensile and burst tests). Therefore, it can not be precluded that high burnup (non-uniformly) hydrided cladding may have lower fracture toughness values than the 5 - 10 ksi√inch range observed for uniformly hydrided Zircaloy.

The above fracture mechanics calculations focus attention on the factors that could influence the uncontrolled pressure driven growth of axial cracks in stored spent fuel. Further work is required to come to definitive conclusions whether the scenario of long axial splits is a physical possibility for the clad dimensions, internal pressures, and material properties. The following summarizes known trends and remaining uncertainties:

1. an improved understanding of dynamic crack growth in clad could have significant benefits in resolving uncertainties in potential break sizes and radiological releases,
2. there have been no reported occurrences of long axial splits in fuel clad for the conditions that exist (static internal pressure) during the storage of spent fuel; regulatory concerns about this postulated failure mode appear to be caused by a few long axial splits of clad that have occurred during operation; these failures have been driven by high stresses caused by pellet-clad interactions that are not a factor during storage,
3. it is generally believed that flaws in cladding will in most cases cause only through-wall cracks and a loss of the internal pressure by leakage of the fission product gases; once the internal pressure is relieved the potential for large breaks no longer exists,
4. the potential for long axial splits in cladding cannot be precluded by application of conservative criteria for crack arrest that are based solely on the ratio of upper bound velocities for dynamic crack growth to depressurization velocities for the confined gases,

5. the above assessments suggest that relatively low levels of fracture toughness could be sufficient to reduce the crack velocities for axial cracks to such an extent that the fuel rod will depressurize sufficiently to arrest running axial cracks,
6. the above fracture mechanics assessments have very conservatively neglected the effects of the fuel pellets and have assumed that the clad is entirely filled with gas; structural mechanics calculations are recommended to account for the finite volume of pressurized gas; such calculations could show a very large beneficial effect of the low volume of gas and rule out any potential for large axial breaks in spent fuel cladding.

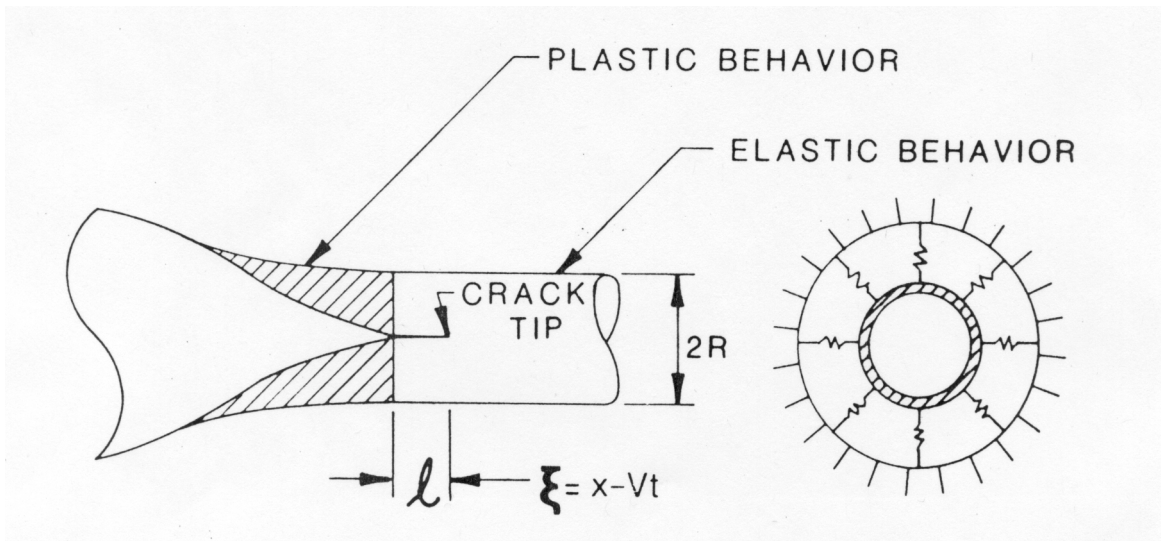


Figure 2-1 Propagation of Axial Crack in a Pressurized Cylinder

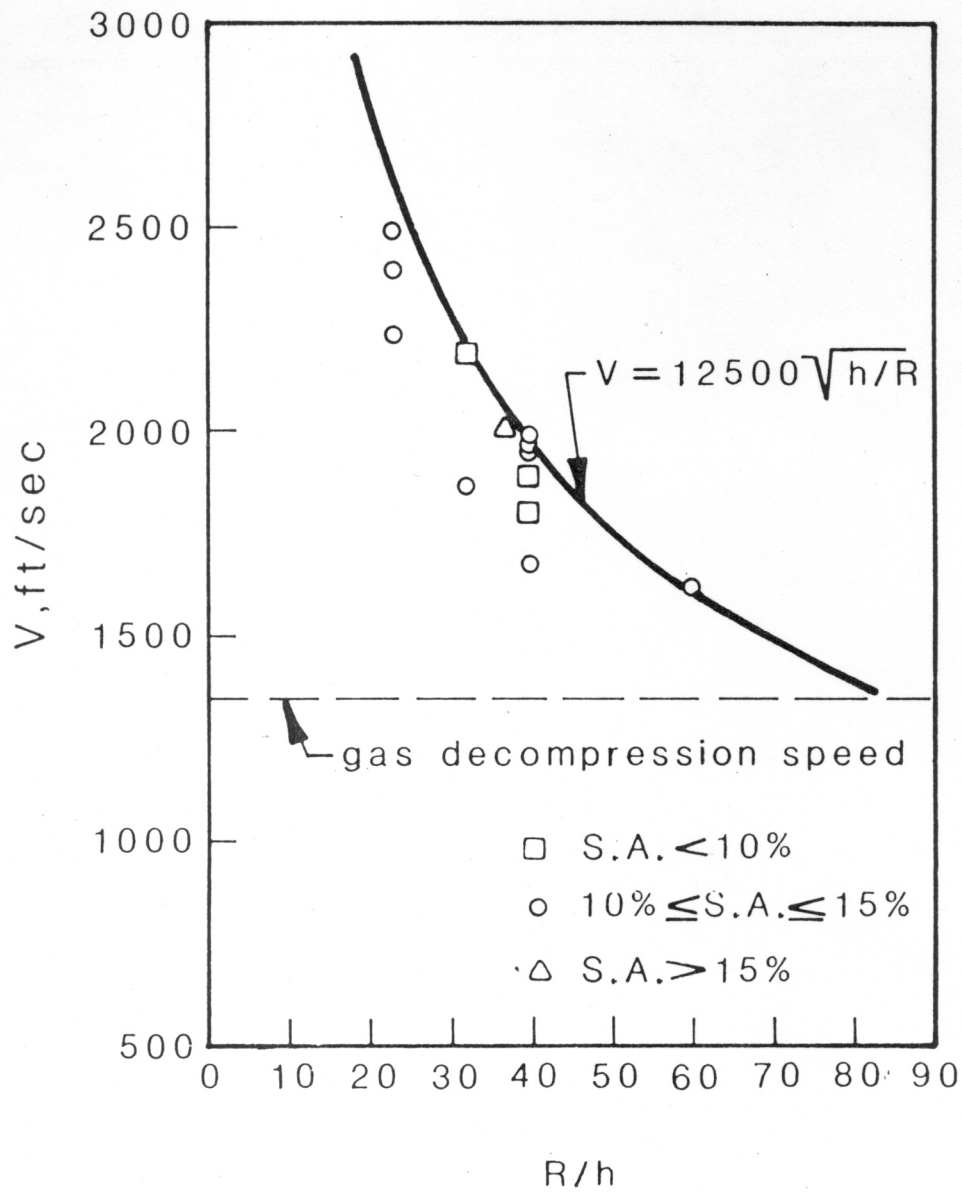


Figure 2-2 Velocities of Crack Propagation and Depressurization Wave

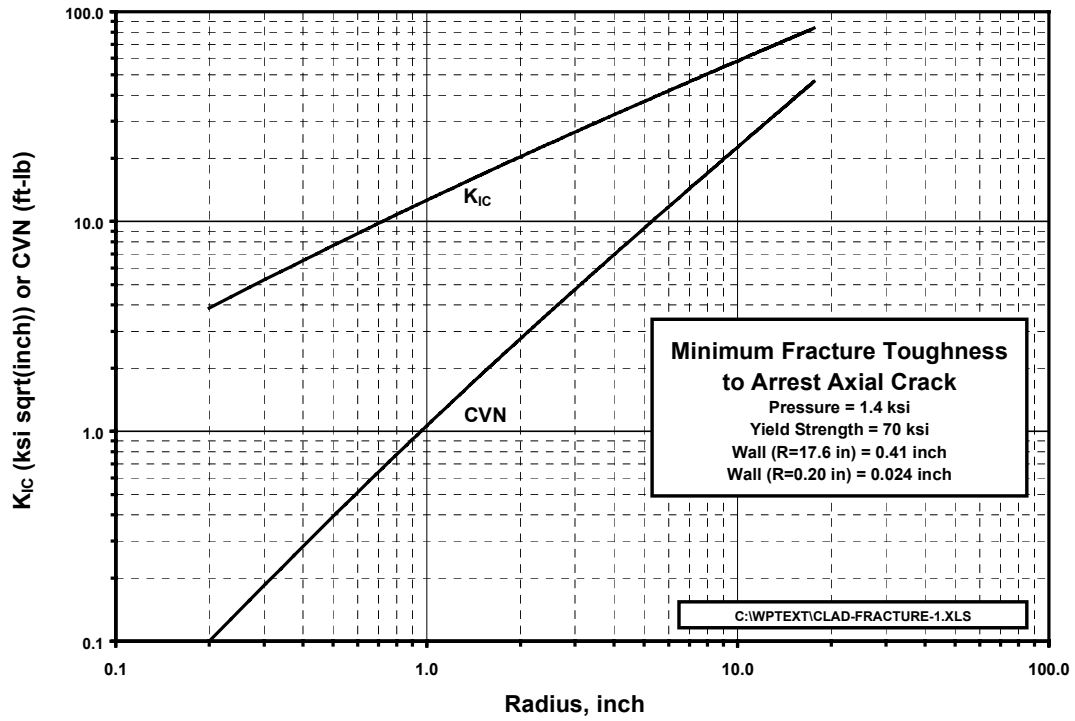


Figure 2-3 Minimum Toughness to Arrest a Running Crack

### 3.0 Through-Thickness Variations in Material Properties

Spent fuel clad after exposure to neutron irradiation and hydride formation will have significant through-thickness variations in material properties. It is observed that a thin oxide layer forms on the outer surface, with a hydride rim forming below the oxide layer. The thickness of this hydrided rim can extend in some cases through 50 percent or greater of the clad wall if spalling and hydride blisters form. The hydrides tend to concentrate at the outer surface because the surface is maintained during reactor operation at a cooler temperature and because hydrogen tends to move to regions of cooler temperatures. The inner 50 percent or more of the wall thickness may also have elevated hydrogen concentrations, but not sufficiently high to support the formation of hydride platelets. PNNL has not seen any data on toughness variations through the wall of the cladding. However, it is reasonable to assume that the outer hydride rim of spent fuel cladding will have relatively low toughness levels, whereas the inner part of the wall will have higher levels of toughness more characteristic of the original unaged condition of the clad material. The reviewed publications (Garde et al. 1996, Hermann 1999, Meyer et al. 1996, Fuketa et al. 1996, Fuketa et al. 2000) on spent fuel cladding shows photographs of outer hydride layers with cracks extending through the hydride rim and with these cracks ending at the inner region of the wall. These publications also show cracks extending completely through the wall, particularly where oxide spallation and large hydride blisters have formed.

The NEI report presents data for clad fracture toughness in terms of hydrogen concentrations that have been averaged through the clad thickness and for fracture tests using specimens that have been prepared to give uniform hydrogen concentrations throughout the volume of the specimen. Such specimens will only approximate the conditions for the propagation of clad cracks. In this regard Kreyns et al. have measured fracture toughness levels in uniformly hydrided and irradiated clad materials that showed considerable scatter. The very lowest toughness (extreme levels of uniform hydrides) was 7.4 MPa√m (6.7 ksi√inch). There were some toughness values in the range of 12 MPa√m (10.9 ksi√inch). More typical toughness values for irradiated/hydrided cladding were in the range of 15-20 MPa√m (13.7-18.2 ksi√inch). The Kreyns tests were for specimens with dimensions of about 1.0 inch – much greater than the wall thickness of the clad. Again it should be noted that the specimens were prepared to achieve hydriding in a uniform manner throughout the volume of the specimens and the ductility of clad with uniform hydrides is generally greater than those observed in high burnup cladding with non-uniform hydrides. The Kreyns data are for both transgranular fractures and intergranular fractures.

Clearly the toughness of high burnup cladding will have different values through the clad wall. The toughness of the hydrided rim is likely to be relatively low, i.e., could approach or be below the lower bound level of 7.4 MPa√m ((6.7 ksi√inch) indicated by the Kreyns data. However, the inner part of the clad wall with lower levels of hydriding should have much better toughness levels.

PNNL performed calculations to address potential effects of through-thickness toughness variations based on the following nominal parameters for spent fuel cladding:

- Clad outer diameter = 0.400 inch
- Clad wall thickness = 0.022 inch
- Hoop stress in clad wall = 15 to 20 ksi (due to internal pressure)
- Thickness of outer hydrided rim = 50 percent of wall

The first set of fracture mechanics calculations considered long axial cracks extending entirely through the thickness of the hydride rim. The crack depth was set equal to  $a = t/2 = 0.022/2 = 0.011$  inch with the possible hoop stress in the clad was assumed to range from 10 to 100 ksi with an expected stress of 20 ksi. Stress intensity factors were calculated from equations in Rooke and Cartwright (page 241) as follows:

Applied Stress, ksi	Applied Stress Intensity Factor, ksi√inch
10	4.34
20	8.68
50	21.7
100	43.4
Expected Clad Stress During Storage 15 - 20	6.5 to 8.7

The lower bound on fracture toughness (as cited above) is 6.7 ksi√inch (7.4 MPa√m) for irradiated Zircaloy with high uniform hydriding. The issue here is that uniformly hydrided Zircaloy (used to establish the minimum fracture toughness) appears to have higher ductility than observed in high burnup cladding that is non-uniformly hydrided (based on tensile and burst tests). Therefore, it cannot be concluded that high burnup (non-uniformly) hydrided cladding may have lower fracture toughness values than the 6.7 ksi√inch range observed for uniformly hydrided Zircaloy. The material inside of the hydrided rim should however have relatively good toughness that is significantly greater than this lower bound value. It can then be concluded that cracks in the hydride rim are unlikely to grow as a sudden brittle fracture through the remainder of the clad wall.

A second failure mode addressed by PNNL is related to blisters (a region of spalled oxide layer). It was assumed that the spalled oxide would locally remove the insulating oxide layer and this would result in a cold spot. If hydrogen concentrates in such a cold spot, hydrogen platelets could form through the entire wall thickness. Accordingly, the fracture mechanics calculations considered an axial through-wall crack extending across the full diameter of the spalled region as indicated in Figure 3-1. The calculations evaluated the stability of this through-wall crack, and the potential for a large breach in the clad.

The nominal hoop stress in the clad wall during dry storage was again taken to be 20 ksi. This stress was conservatively increased to 40 ksi over the full length of the fuel pin to account for possible fractures in the hydride rim extending through the outer 50 percent of the clad wall. The yield strength of the clad material was estimated to be 87 ksi, which is more than two times the assumed 40 ksi hoop stress. Therefore, elastic-plastic effects were not considered to be relevant. Local through-wall axial cracks ranging in length from 0.10 to 0.40 inch were addressed. These cracks corresponded at one extreme to a small crack spanning a blister diameter of 5 times the wall thickness and at the outer extreme to a long crack spanning a full blister diameter equal to the clad diameter. From Rooke and Cartwright the following stress intensity factors were calculated:

Blister Diameter	Length of Axial Crack, inch	Applied Stress Intensity Factor, ksi√inch
5 times tube wall thickness	0.10	26.2
50 percent of tube diameter	0.20	53.8
100 percent of tube diameter	0.40	104.6

These stress intensity factors (even for the smallest crack) could exceed the fracture toughness of the relatively tough material of the clad inside of the hydride rim. Therefore, there is a potential for unstable growth of axial cracks if: 1) the blister diameter becomes sufficiently large, and 2) the full wall thickness becomes severely hydrided over this region. The calculations also assumed that a long axial crack forms within the blister, and that this crack penetrates the clad with no opportunity for a slow leak to relieve the internal gas pressure. Actual fuel rod behavior may be such that through-wall cracks could result in a slow leak rather than a long break. However, the simple calculations in Section 2.0 show that crack propagation is possible and that further analysis is needed. The final length of the axial fracture will depend on how rapidly the gas pressure is released compared to the velocity of crack propagation.

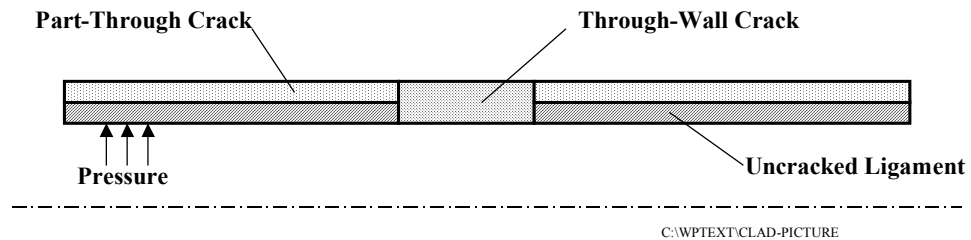


**Figure 3-1 Clad with Through-Wall Crack at Blister**

#### 4.0 References

Electric Power Research Institute. 2001. *Fracture Toughness Data for Zirconium Alloys – Application to Spent Fuel Cladding in Dry Storage*, Technical Progress Report 1001281, Albert J. Machiels – EPRI Project Manager, January 2001.

Electric Power Research Institute. 2000. *Creep as the Limiting Mechanism for Spent Dry Storage*, Technical Progress Report 1001281, Albert J. Machiels – EPRI Project Manager, December 2000.

Kanninen, M.F. and C.H. Popelar. 1985. *Advanced Fracture Mechanics*, Oxford University Press, New York.

McGuire, P.A., S.G. Sampath, C.H. Popelar and M.F. Kanninen. 1980. "A Theoretical Model for Crack Arrest in Pressurized Pipelines," *Crack Arrest Methodology and Applications, ASTM STP 711*, G.T. Hahn and M.F. Kanninen, Eds., American Society of Testing and Materials, pp. 341-358.

Rolfe, S.T. and J.M. Barsom. 1977. *Fracture and Fatigue Control in Structures – Applications of Fracture Mechanics*, Prentice-Hall, Inc. Englewood Cliffs, New Jersey.